Electric-Power-Steering system Vehicle Control Stability and Return Strategies Based on Predictive Control

Shi Songzhuo* and Chen Guangda

School of Electrical and Information Engineering, Beihua University, Jilin 132013, China

_____

Abstract

Steering wheel torque may fluctuate when vehicles are making a steering return. Variation of steering wheel return torque may lead to insufficient or excessive return of vehicles, thereby influencing the steering stability of vehicles. To disclose the relationship between the performances of Electric-Power-Steering (EPS) system and vehicle control stability, a return control strategies for the entire vehicle EPS system based on predictive control algorithm was proposed. The state equation that combines the EPS system and the whole vehicle was built up through system modeling, and discretized thereafter. An EPS system-based vehicle predictive control model was constructed based on the objective yaw rate. Moreover, a system model based on the combination of MATLAB and CarSim software was constructed. Optimal values of parameters of the prediction system were determined by analyzing parameter characteristics in the predictive model. Return performances of the EPS system was improved by adjusting the power dead zone value, during which steering wheel torque signal was used as a control parameter. Validity of the predictive model and return control strategy was verified through a simulation experiment and field test. Results demonstrate that the designed control system can effectively improve control stability of vehicles and strengthen return of system. Yaw rate response time of vehicles after optimization of the control and prediction time domains in the predictive control is decreased by 4 s and the response amplitude decreased by 2 deg compared with those before optimization. The minimum return residual angle of steering wheel is 2.2 deg. The proposed method provides significantly references to explore the vehicle control stability and return control strategy of EPS.

Keywords: Electric-Power-Steering System, predictive control, vehicle control stability, return control

_____

1. Introduction

Electric-power-steering (EPS) system has become the most primary safety component in the steering system of vehicles. Performance reliability of an EPS system is related to the control stability of the whole vehicle [1]. Return control is the main function of an EPS system. If the return performance of vehicles is poor, then drivers have to rotate and continuously adjust the steering wheel angle to maintain the vehicles' straight traveling, thereby easily causing driving fatigue. Consequently, this situation may trigger driver complaints and even result in potential safety hazards [2]. As vehicle driving system develops toward high integration, vehicle development focuses on improved safety and comfort, and the safety level of steering systems increases gradually. To strengthen the control stability of vehicles, the vehicle modeling integration of EPS system increases and the control strategy involves multiple factors, thereby bringing immense challenges to conduct research on the EPS system.

On this basis, studies on the subsystem control of vehicles are independent research, which do not consider mutual influences among subsystems. The complicated driving conditions of vehicles and complicated variation laws of self-return torque of vehicles present considerable challenges to the design of return control strategy and real vehicle experiment [3,4]. Li et al. demonstrated that there are many uncertain factors in the whole vehicle modeling of the EPS system. Moreover, inexplicit factors of return control

strategy decrease the control stability of the system [5], but there are still accuracy problems in the EPS system modeling and stability of control strategy. Therefore, determining a more accurate EPS of the whole vehicle model and establishing a control strategy of the EPS system to strengthen the control stability of whole vehicles are problems that should be solved urgently.

Therefore, a predictive control model of vehicle EPS was constructed using the system modeling method to analyze the parameters of prediction and control time domains of the models and yaw rate. This model aims to accurately control return current and return residual angle of the system, thereby providing references to improve the control stability of vehicles.

The preceding results mainly focus on EPS, and a single EPS system model simulation was the major research method. The motor control strategy mainly used assist control. Only a few studies have been conducted on the whole vehicle model of EPS, particularly research on control strategy of the vehicle EPS. Accordingly, an algorithm for predictive control based on state equation was applied by using the ideal yaw state of vehicles as reference to establish a vehicle nonlinear discrete model of EPS. In this study, yaw rate of the whole vehicle was used as optimization object. Influences of predictive and control time domains on assist current and yaw rate of the whole vehicle in the predictive control model under different ideal yaw rates were analyzed to improve stability of steering wheel holding by drivers. Moreover, a return control strategy was designed through the steering wheel torque signal detected by torque sensor in the EPS system to provide references in improving the control stability of vehicles.

The reminder of this study is organized as follows. Section 2 gives the relevant background, including related work on control strategy of EPS system. Section 3 constructs a predictive control model of vehicle EPS. On the basis of this model, a return control strategy of EPS was constructed and the optimization strategy of predictive control parameters based on fuzzy rules was formulated. Section 4 analyzes the return performances and control stability of vehicles by using the control model of vehicle EPS. Relationships are disclosed between return torque and vehicle speed under different working conditions, as well as influences of different predictive control parameters on vehicle control stability. Section 5 summarizes and provides the conclusions.

2. State of the art

EPS is mainly studied by establishing the system dynamic model, and the motor control strategy mainly assists the control and return control modes. To date, numerous studies have been conducted on the control strategy of EPS. Na [6] designed a motor torque control strategy based on the active disturbance rejection (ADR) algorithm to strengthen the robustness of EPS under low-frequency disturbances, such as road resistance and irregular mechanical friction. However, he did not explore EPS and the whole vehicle. Chen [7] designed an EPS based on permanent magnet synchronous motor for all-terrain vehicles and predicted control current by using the vector model, thereby effectively decreasing current ripples and increasing the current response speed of the system. However, return performances of the system was not considered. To provide drivers with better driving comfort, Li [8] designed a double-motor EPS and its working reliability was verified through lemniscate and step tests. Nevertheless, uncertainty of system modeling was not considered. Ding [9] improved the vehicle control stability of the EPS system using the genetic algorithm, particularly by adjusting the reduction ratio of decelerating mechanism.

Wang [10] studied the electro-hydraulic coupling steering system and determined the ideal steering wheel torque of drivers based on vehicle speed and lateral acceleration by using the ADR control strategy. However, he did not involve studies on the control stability of the whole vehicle system. To improve the reliability of the EPS system, Ma [11] proposed the reliability modeling and assessment methods of the EPS system based on the model driving structure, and constructed a method for system reliability assessment by using structural analysis and design language. Shang [12] used a light truck as carrier and investigated the system convenience of the mode under the assistance of the EPS system by using the fuzzy adaptive PID control strategy, and verified the reliability of the control strategy through a simultaneous platform. However, this research did not involve studies on return condition of EPS. Yoshiyuki Yasui et al. estimated road adhesion coefficient through return torque of tires, and shared it with other systems[13,14]. Chen et al. proposed an EPS return control strategy based on fuzzy nonlinear state error feedback strategy, and processed the return control parameter fuzzy. This control algorithm did not rely on the mathematical model of objects, and the control system had strong robustness [15]. Wang et al. designed a return control strategy of EPS, which uses the sideslip angle of vehicles as judgment reference. They connected return performances of the EPS system with the whole vehicle performances [16]. Du [17] proposed a complete active return control strategy for the EPS system. To avoid sudden changes

of the output torque of the drive motor, a disturbance-free switching logic algorithm was designed.

3. Methodology

3.1 EPS modeling
As shown in Fig. 1, EPS includes a mechanical steering system, torque sensor, assist motor, and ECU controller.
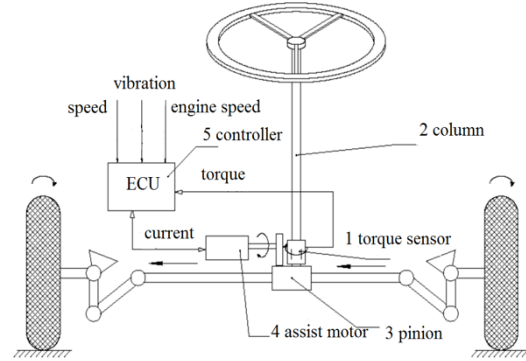

Fig. 1. Schematic of EPS

According to the dynamic relations of steering system, the state equation model of ESP was established; system state variables were $x=\left[\begin{array}{ccccccc} \theta_s & \ddot{\theta}_s & x_r & \ddot{x}_r & \theta_m & \ddot{\theta}_m & i \end{array}\right]$, input variables were $u=[\begin{array}{ccc} T_d & U & T_w \end{array}]^T$, and output variables were $y=[\begin{array}{cccc} T_a & i & T_s & \theta_s & \ddot{\theta}_m \end{array}]$. The system state equation is expressed as follows:

$$\dot{x} = Ax + Bu$$
$$y = Cx + Du \tag{1}$$

$$A=\begin{bmatrix} 0 & 1 & 0 & 0 & 0 & 0 & 0 \\ -\dfrac{k_s}{J_s} & -\dfrac{k_s}{J_s} & \dfrac{k_s}{rJ_s} & 0 & 0 & 0 & 0 \\ 0 & 0 & 0 & 0 & 0 & 0 & 0 \\ \dfrac{k_s}{rm_r} & 0 & -\dfrac{k_s+k_mG^2}{r^2m_r} & -\dfrac{b_r}{m_r} & \dfrac{k_mG}{rm_r} & 0 & 0 \\ 0 & 0 & 0 & 0 & 0 & 1 & 0 \\ 0 & 0 & \dfrac{k_mG}{rJ_m} & 0 & -\dfrac{k_m}{J_m} & -\dfrac{b_m}{J_m} & 0 \\ 0 & 0 & 0 & 0 & 0 & -\dfrac{k_f}{L} & -\dfrac{R}{L} \end{bmatrix}$$

$$B=\begin{bmatrix} 0 & 0 & 0 \\ \dfrac{1}{J_s} & 0 & 0 \\ 0 & 0 & 0 \\ 0 & 0 & -\dfrac{1}{m_r} \\ 0 & 0 & 0 \\ 0 & 0 & 0 \\ 0 & \dfrac{1}{L} & 0 \end{bmatrix}$$

$$C=\begin{bmatrix} 0 & 0 & -\dfrac{k_mG}{r} & 0 & k_m & 0 & 0 \\ 1 & 0 & 0 & 0 & 0 & 0 & 0 \\ 0 & 0 & 0 & 0 & 1 & 0 & 0 \\ 0 & 0 & 0 & 0 & 0 & 0 & 1 \\ k_s & 0 & -\dfrac{k_s}{r} & 0 & 0 & 0 & 0 \end{bmatrix}$$

$$D = [0].$$

where K_s is the stiffness coefficient of bar of torque sensor, r is the radius of pinion, K_m is the equivalent stiffness coefficient of motor and decelerating mechanism, G is the speed-up ratio of turbine worm, m_r is the mass of steering tie rod, b_m is the viscous friction coefficient of motor, J_m is the rotational inertia of motor, L is the inductance of motor armature, R is the resistance of motor armature, θ_s refers to the rotating angle of the steering wheel, x_r refers to the displacement of rack, θ_m is the rotating angle of motor, i is the current of the motor, T_d is the input torque of steering wheel, U is the voltage of motor end, T_w is the anti-torque acting on the steering output shaft, T_a is the assist torque output by the motor, and T_s is the output torque of the torque sensor.

3.2 Assist characteristics of the EPS system
The designed assist curve is the straight assist curve. The assist characteristic curve of the straight EPS system is shown in Fig. 2. Accordingly, when the steering torque detected by EPS changes within the regulated range, there is a linear relationship between the assist current of the motor and steering wheel torque. The straight assist characteristic mode has simple programming and convenient for modification. Variation curves of the input-output torques of EPS with vehicle speed are shown in Fig. 3.
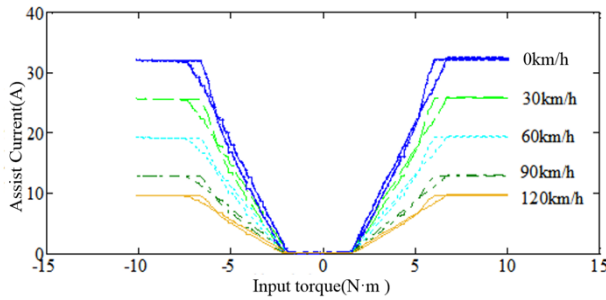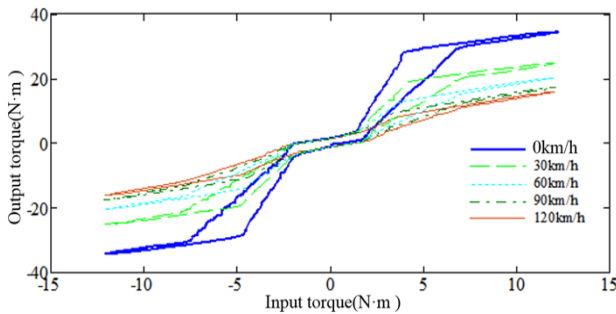

Fig. 2. Straight assist characteristic curves

Fig. 3. Variation curves of the input–output torque with vehicle speed

3.3 Construction of the prediction model of vehicle EPS

To study the influences of EPS on the yaw rate of vehicles, a 2-degree-of-freedom (DOF) steering model of the whole vehicle (Fig. 4) was used. This model hypothesizes that the vehicle makes planar motions parallel to the ground, and the differential equation of motion of the model is shown as follows:
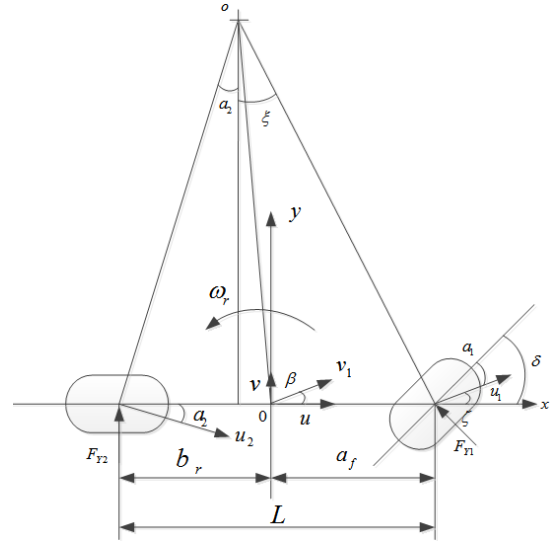

Fig. 4. Two-DOF vehicle model

$$-2k_1 \cdot \beta + \frac{a_f \omega_r}{u} - \delta 2k_2 \cdot (\beta - \frac{b_f \omega_r}{u}) = m(\dot{v} + u\omega_r)$$

$$-2a_f k_1 \cdot (\beta + \frac{a_f \omega_r}{u} - \delta) + 2b_f k_2 \cdot (\beta - \frac{b_f \omega_r}{u}) = I_z \dot{\omega}_r \quad (2)$$

where m is the mass of vehicles, a_f is the distance from front wheel to the centroid, b_f is the distance from rear wheel to the centroid, I_z refers to the rotational inertia of the vehicle around the Z-axis, B is the sideslip angle, and ω_r is the yaw rate of vehicles.

During normal driving of vehicles, lateral acceleration is no higher than 0.4 g and the slip angle of tire is no larger than 5 deg. In this circumstance, the sideslip force of tire (F_r) has a linear relationship with the sideslip angle (a). In this case, the linear tire model can be used, and T_r is the return torque. The function description is as follows [18]:

$$T_r = -2k_1 \cdot (\beta + \frac{a_f \omega_r}{u} - \delta) \cdot d = K_T \cdot \delta$$

$$K_T = 2k_1 - 2k_1 \cdot A_1 \cdot a_f / u - 2k_1 \cdot A_2 \quad (3)$$

Combining with the differential equation of motion of EPS and the 2-DOF vehicle motion equation, a comprehensive model consisting of the EPS, vehicle steering, and tire models was constructed. Moreover, $X = [\dot{\theta}_s \ \ddot{\theta}_s \ \dot{\theta}_p \ \theta_p \ \omega_r \ \beta]^T$ was defined as the state vector of the model system, $u = [T_s \ i]^T$ as the input vector of the system, and $Y = [T_{det} \ \omega_r]^T$ as the output variable. The combined system state equation is as follows:

$$\ddot{\theta}_s = -\frac{B_s \dot{\theta}_s}{J_s} - \frac{K_{TS}\theta_s}{J_s} + \frac{K_{TS}\theta_P}{J_s} + \frac{T_s}{J_s}$$

$$\ddot{\theta}_P = 1/(\frac{J_2}{k_e^2} + J_m k_m^2) \cdot (-(\frac{B_2}{k_e^2} + B_m k_m^2)\dot{\theta}_P - (\frac{2k_1 d}{k_e^2} + K_{TS})\theta_P$$

$$+ K_{TS}\theta_s + \frac{2k_1 d a_f}{uk_e}\omega_r + \frac{2k_1 d}{k_e}\beta + k_m K_f i) \quad (4)$$

$$\dot{\omega}_r = \frac{2a_f k_1}{I_z k_c}\theta_P - \frac{2a_f^2 k_1 + 2b_r^2 k_2}{I_z u}\omega_r - \frac{2a_f k_1 - 2b_r k_2}{I_z}\beta$$

$$\dot{\beta} = \frac{2k_1}{muk_c}\theta_P - (1 + \frac{2a_f k_1 - 2b_r k_2}{mu^2})\omega_r - \frac{2(k_1 + k_2)}{mu}\beta$$

The state equation that combines the whole vehicle and EPS is a nonlinear model. To adapt to the predictive controller, linearization of the model is needed first. The state equation of the model that combines the whole vehicle and EPS can be written as follows:

$$\dot{\xi}_{dyn} = f_{dyn}(\xi_{dyn}, u_{dyn}) \tag{5}$$

where ξ_{dyn} is the state variable and u_{dyn} is the control variable.

The state equation of the model that combines the whole vehicle and EPS has Taylor series expansion at any point. The first-order term is retained [19], while high-order terms are disregarded, thereby obtaining the following linear time-varying equation:

$$\dot{\xi}_{dyn} = A_{dyn}(t)\xi_{dyn}(t) + B_{dyn}(t)u_{dyn}(t)$$
$$\dot{\varepsilon}_{dyn} = C_{dyn}(t)\xi_{dyn}(t) + D_{dyn}(t)u_{dyn}(t) \tag{6}$$

where $A_{dyn}(t) = \frac{\partial f_{dyn}}{\partial \xi_{dyn}}\big|_{\xi, u}$, $B_{dyn}(t) = \frac{\partial f_{dyn}}{\partial u_{dyn}}\big|_{\xi, u}$ $C_{dyn}(t) = \frac{\partial f_{dyn}}{\partial \xi_{dyn}}\big|_{\xi, u}$

Given that the equation is a continuous linear equation, discretization is needed to use in the design of predictive controller in the model. The state equation of the model that combines the whole vehicle and EPS is approximately discretized as follows:

$$\frac{\xi_{dyn}(t+T^*) - \xi_{dyn}(t)}{T^*} = A_{dyn}(t)\xi_{dyn} + B_{dyn}(t)u_{dyn} \tag{7}$$

where $A_{kin} = I^{\bullet} + T^{\bullet}A(t)$.
$B_{kin} = T^{\bullet}B(t)$

A nonlinear system after linearization at any reference point was gained. This system is the basis for the design of predictive control algorithm of a linear model. In this study, a discrete linear time-varying state equation was gained through preceding linearization of the nonlinear dynamic model of vehicles.

$$\xi_{kin}(k+1) = A_{kin}(k)\xi_{kin}(k) + B_{kin}(k)u_{kin}(k)$$

The basic principle of model's predictive control can reflect three major components of the vehicle predictive control system from three elements of the algorithm: predictive model, rolling optimization, and feedback correction. The three major components of the system are the predictive control algorithm, EPS, and CarSim vehicle system modules. The framework of the vehicle predictive control is shown in Fig. 5.
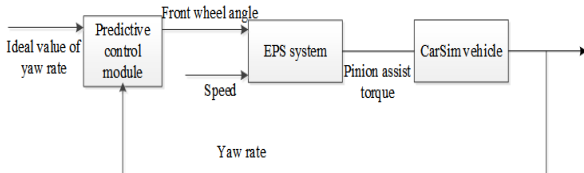

Fig. 5. Framework of the vehicle predictive control

The discrete state space model of EPS and vehicle model are shown as follows:

$$\dot{\tilde{\xi}}_{kin}(k+1) = A_{kin}(k)\tilde{\xi}_{kin}(k) + B_{kin}(k)\tilde{u}_{kin}(k)$$
$$\tilde{\varepsilon}_{kin}(k+1) = C_{kin}(k)\tilde{\xi}_{kin}(k) + D_{kin}(k)\tilde{u}_{kin}(k) \tag{8}$$

Augmentation state variable is set as follows:

$$\xi(k) = [\, x(k)\quad u(k-1)\,]^T \tag{9}$$

The new state space expression of the system is as follows:

$$\xi(k+1) = \tilde{A}_{kin,t}(k)\xi_{kin}(k) + \tilde{B}_{kin,t}(k)\Delta\tilde{u}_{kin}(k)$$
$$\eta(k) = \tilde{C}_{kin,t}(k)\xi_{kin}(k) \tag{10}$$

where the state matrixes are defined as follows:

$$\tilde{A}_{kin,t} = \begin{bmatrix} A_{kin,t} & B_{kin,t} \\ 0 & I \end{bmatrix}$$
$$\tilde{B}_{kin,t} = \begin{bmatrix} B_{kin,t} \\ I \end{bmatrix}$$
$$\tilde{C}_{kin,t} = \begin{bmatrix} C_{kin,t} & 0 \end{bmatrix}.$$

Suppose:

$$\tilde{A}_{kin,t} = \tilde{A}_t, k = 1, \cdots, t+N-1$$
$$\tilde{B}_{kin,t} = \tilde{B}_t, k = 1, \cdots, t+N-1$$

If the predictive and control time domains of the system are N_p and N_c, respectively, the state variable in the predictive time domain and system output can be calculated using the following equation:

$$\xi(t+N_p) = \tilde{A}_{kin,t}^{N_p}(k)\xi(t) + \tilde{A}_t^{N_p-1}(k)\tilde{B}_{kin,t}(k)\Delta\tilde{u}_{kin}(t) + \cdots$$
$$+ \tilde{A}_t^{N_p-N_c-1}\tilde{B}_{kin,t}(k)\Delta\tilde{u}_{kin}(t+N_c)$$
$$\eta(t+N_p\tilde{C}_{kin,t}\tilde{A}_{kin,t}^{N_p}\xi_{kin}(t)\tilde{C}_{kin,t}\tilde{A}_{kin,t}\tilde{B}_{kin,t}(k)\Delta\tilde{u}_{kin}(t)$$
$$+ \cdots + \tilde{C}_{kin,t}\tilde{A}_{kin,t}^{N_p-N_c-1}\tilde{B}_{kin,t}(k)\Delta\tilde{u}_{kin}(t+N_c) \tag{11}$$

The expected yaw rate under the ideal state of vehicles is as follows:

$$\omega_{rd} = \frac{v_x/L}{1 + \frac{m}{L^2}(\frac{L_f}{C_{lf}} - \frac{L_r}{C_{lr}})v_x^2} \cdot \delta = \frac{v_x/L}{1 + Kv_x^2} \cdot \delta \tag{12}$$

where v_x is the longitudinal acceleration of vehicles along the longitudinal axis, L_f is the distance from the center of gravity to the front axis, L_r is the distance from the center of gravity to the rear axis, C_{lr} is the lateral stiffness of the tire, and C_{lf} is the longitudinal stiffness of the tire.

Linear optimization of control parameters in the predictive controller was performed using the fuzzy controller. Inputs of the fuzzy regulator were yaw rate error of vehicles and its variation rate.

Fuzzy function was operated in the command window of MATLAB and entered into the fuzzy logic editor. A new FIS file was established and the controller type Mamdani was chosen. According to the preceding analysis, membership function and quantized interval of $e = 0.5$ and $de = 0.5$ were input. Fuzzy control rules were input in the form of "If…then," thereby establishing an FIS document. Inference results of the control domain (N_c) and predictive time domain (N_p) were gained. Inference results of N_c and N_p when are shown in Fig. 6, where $N_c = 4$ and $N_p = 10$.
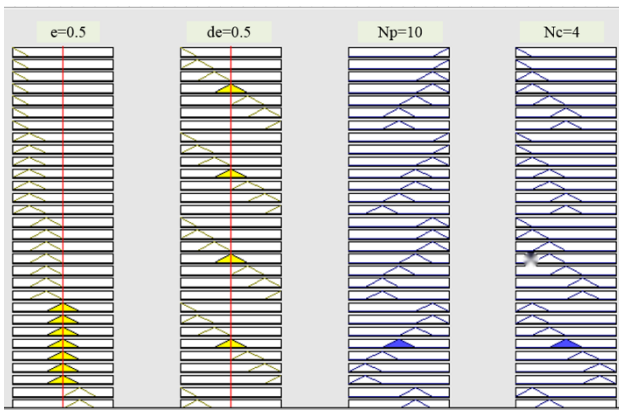
Fig. 6. View of the fuzzy rules

3.4 Return control strategy

Without increasing hardware cost of the system, angle sensor was not added in the EPS system. The return controller determines whether or not the system is in the return condition by judging variations of the steering wheel torque detected by the torque sensor. The return control process is introduced as follows. When a vehicle finishes the steering, the driver releases the steering wheel, which moves toward its center point driving by the return torque. Owing to the existence of system resisting torque, the steering wheel cannot return to the center point accurately under the driving force of the return torque. Hence, an extra return torque has to be applied to the steering wheel to make it accurately return to the center point. The working state of EPS is determined according to variations of steering wheel torque, assist current, and holding time. In an ideal state, the system is in the return state when assist current is zero, steering wheel torque is smaller than T_{dead}, and the state holding time is longer than the threshold time (t_q). The steering wheel torque is gained by the torque sensor and the assist current is measured from the PWM value at the metal-oxide-semiconductor field-effect transistor (MOSFET) output end of the system controller. Moreover, T_{dead} is the steering wheel torque when there is no system assist. The logic framework of the return control strategy is shown in Fig. 7.
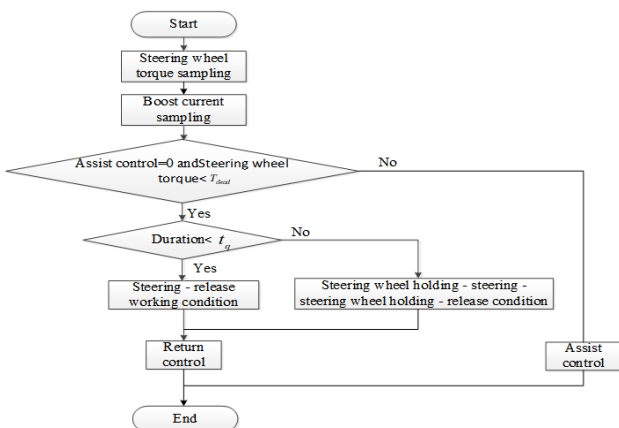

Fig. 7. Logic framework of the return control strategy

The return current is determined by vehicle speed, steering wheel holding time, and steering torque. By calculating the variation of input torque, it is the assist control when the input torque slope increases. It is the return state when the variation rate of the input torque decreases and the assist current is zero. The return current was fit: the return current curve in the input torque-output current curve has to be fit. The current function of return control is as follows:

$$I_{return} = k_p \cdot T_{dead} \cdot F(T_s) \tag{13}$$

where I_{return} is the return current, k_p is the gain coefficient of return current, and FT_s is the steering wheel torque coefficient.

4 Result analysis and discussion

Performances of the designed control strategy were verified by the test bed and the whole vehicle. The performance test bed of EPS is shown in Fig. 8. The experimental apparatus of the whole vehicle is shown in Fig. 9, which includes the testing vehicle, upper computer, debugger, controller, torque and angle testing steering wheel, and oscillograph.

Fig. 8. Performance test bed of EPS

(a) Debugging equipment

(b) Testing vehicle
Fig. 9. Experimental apparatus of the whole vehicle

4.1 Relationship of return current and residual angle with vehicle speed and steering conditions

The steering process of a physical vehicle was simulated. A 10-N•m steering torque was applied to the steering wheel at 2 s, which was held for 0.5 s and released thereafter. In this way, response curve of the steering wheel angle and variation curve of current whether or not there is return control were gained. Return residual angles of the steering wheel at vehicle speeds of 0 and 80 km/h are shown in Figs. 10 and 12, respectively.
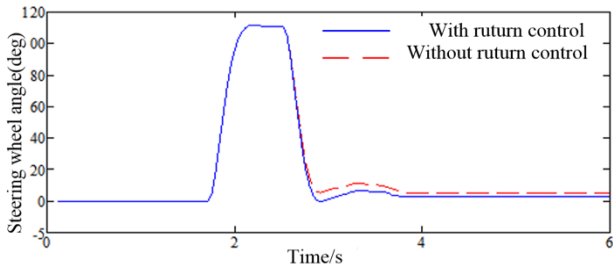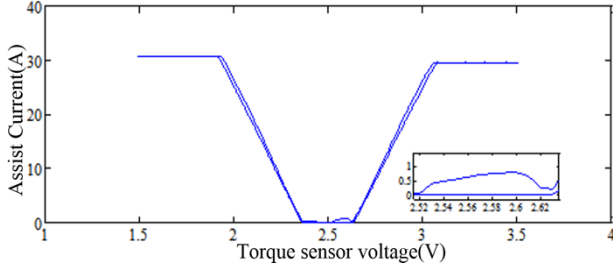
Fig. 10. Return residual angle at 0 (km/h)

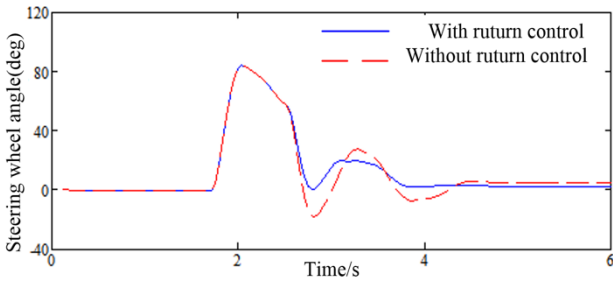

Fig. 11. Return current at 0 (km/h)

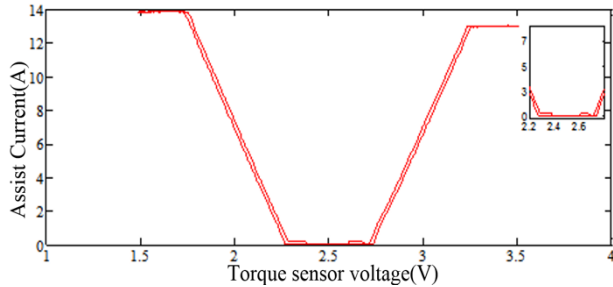**Fig. 12.** Return residual angle at 80 km/h

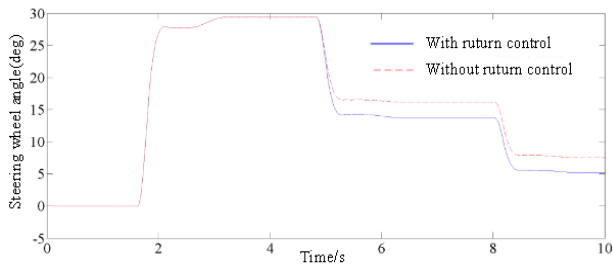
Fig. 13. Return current at 80 km/h

Fig. 14. Steering wheel holding-release-steering wheel holding-release
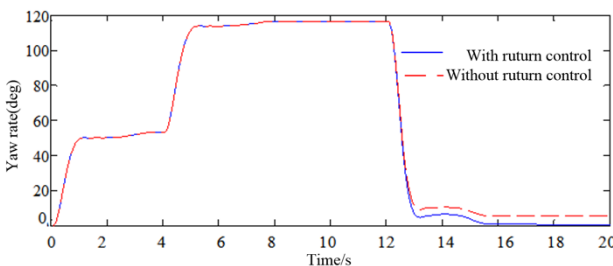

Fig. 15. Steering wheel holding-steering-steering wheel holding-release

Table.1. Parameters of return performances

Vehicle speed (km/h)	Return time (s)		Return residual angle (deg)	
	With return control	Without return control	With return control	Without return control
0	2.4	2.7	7	10
80	2.2	2.8	8	15

Table 1 shows that when vehicle speed is 0, EPS with return control can return in 2.4 s and return residual angle is 7 deg. By contrast, EPS without return control can return in 2.7 s and return residual angle is 10 deg. At vehicle speed of 80 km/h, EPS with return control can return in 2.2 s and return residual angle is 8 deg. By contrast, EPS without return control can return in 2.8 s and return residual angle is 15 deg, accompanied by excessive return.

Variation curves of return currents at 0 and 80 km/h are shown in Figs. 11 and 13, respectively. As shown in Fig. 11, return current is 0.8A at 0, which is attributed to the significant friction resistance of the system. As shown in Fig. 13, to protect the operation stability of the vehicle, return current at 80 km/h decreases by 0.3-0.5 A compared with that at 0. As shown in Fig. 14, under the steering wheel holding-release-steering wheel holding-release condition, residual angle of the steering wheel decreases to 8 deg after adding the return control. Moreover, Fig. 15 shows that under the steering wheel holding-steering-steering wheel holding-release condition, residual angle of the steering wheel decreases to 5 deg after adding the return control.

4.2 Relationship between predictive control parameters and control stability of vehicles
A comparison of the vehicle yaw rate under the step input of the steering wheel torque before and after the optimization is shown in Fig. 16. Yaw rate response time after optimization is 4 s earlier than that before, and fluctuation amplitude decreases by 2 deg.
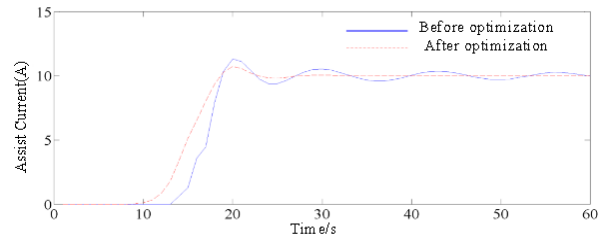

Fig. 16. Comparison of yaw rate before and after optimization

Response curves of yaw rate and assist current of the system under step input of steering wheel (i.e., $N_c = 4$ and $N_p = 2, 5, 10$) are shown in Fig. 17. When $N_p = 2$, Fig. 17 (a) shows that the yaw rate of the vehicle responded the fastest (17 s), but it is accompanied with significant overshooting. Fig. 17 (b) shows that the assist current of the system fluctuates substantially and debugging time is long. When $N_p = 5$, Fig. 17 (a) shows that vehicle yaw rate responded slowly (23 s) but overshooting is small. Moreover, Fig. 17 (b) shows that the assist current of the system fluctuates substantially, and debugging time is short. When $N_p = 10$, Fig. 17 (a) shows that vehicle yaw rate responded rapidly (22 s), with moderate overshooting. Fig. 17 (b) shows that assist current of the system fluctuates slightly, and debugging time is short.
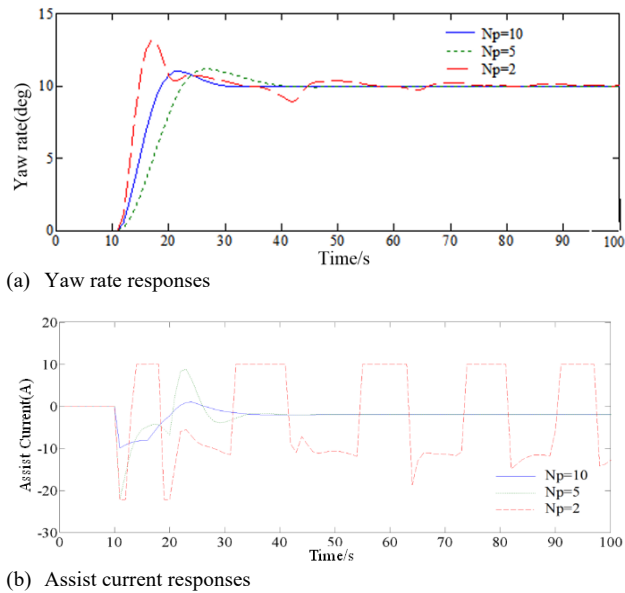
(a) Yaw rate responses

(b) Assist current responses

Fig. 17. System responses at $N_c = 4$

Response curves of yaw rate and assist current of the system under step input of the steering wheel (i.e., $N_p = 10$ and $N_c = 4, 8, 12$) are shown in Fig. 18. When $N_c = 12$, Fig. 18 (a) shows that vehicle yaw rate responded the most slowly (82 s), accompanied with maximum overshooting. Fig. 18 (b) shows that assist current of the system fluctuates significantly, and debugging time is long. When $N_c = 8$, Fig. 18 (a) shows that vehicle yaw rate responded slowly (33 s) but overshooting is small. Fig. 18 (b) shows that assist current of the system fluctuates significantly, and debugging takes a long time. When $N_c = 4$, Fig. 18 (a) shows that vehicle yaw rate responded rapidly (20 s), with moderate overshooting. Fig. 18 (b) shows that assist current of the system fluctuates slightly, and debugging time is short.
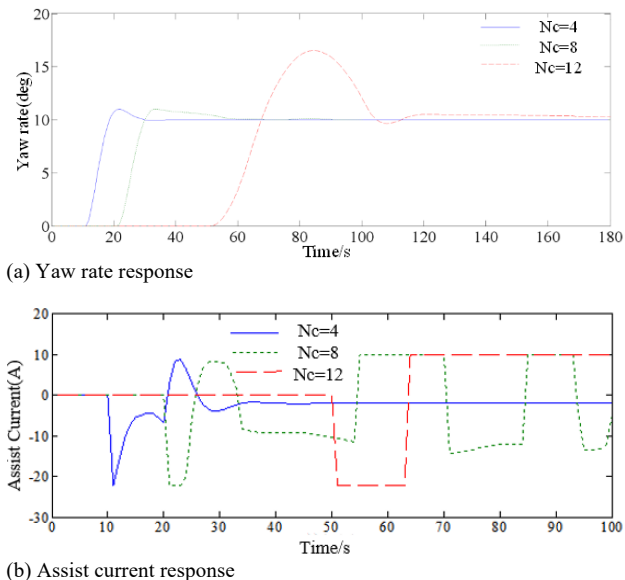

(a) Yaw rate response

(b) Assist current response

Fig. 18. System responses at $N_p = 10$

Yaw rate and assist current comparison curves of the vehicle when the system control input adds limitations and not under step input of steering wheel are shown in Figs.19 (a) and (b), respectively. After the system control input adds limitations, Fig. 19 (a) shows that vehicle yaw rate responded rapidly, fluctuation is small, and debugging time is short. Moreover, Fig. 19 (b) shows that overshooting of assist

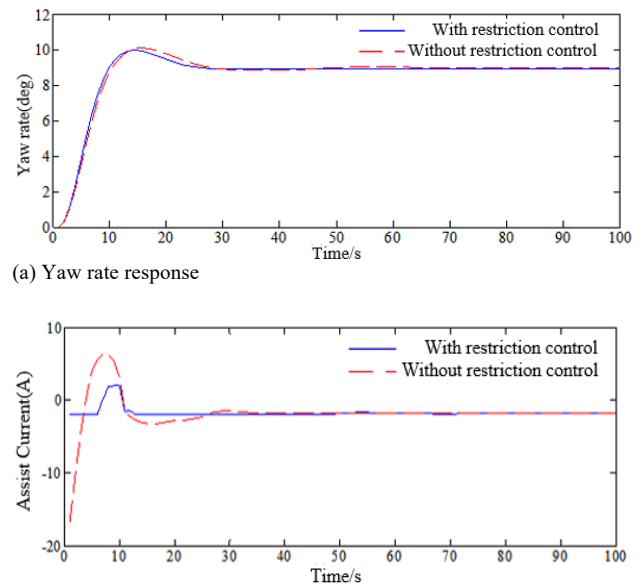current decreases and the debugging time is shortened significantly.

(a) Yaw rate response

(b) Assist current responses

Fig. 19. Comparison of influences of limitations on the system

5. Conclusions

To improve the vehicle control stability of EPS and disclose the relationship of control stability of vehicles with return control current and predictive control parameters, this study constructed a 2-DOF model of the whole vehicle based on EPS. On the basis of this model, a discrete state model of the system was derived. Moreover, a predictive control algorithm of the whole vehicle was established using the yaw rate of vehicles as objective. Effects of the control and predictive time domain parameters of the algorithm on the output responses of the system were analyzed. Moreover, a fuzzy return control strategy of EPS was designed using the steering wheel torque signal as reference. The following conclusions are drawn.

(1) Response time of yaw rate is 4 s earlier after the optimization of the control and predictive time domains in the predictive control compared with that before, and the response amplitude decreases by 2 deg. When the control and predictive time domains are 4 and 10, respectively, the system achieves an optimal control state, manifested by the shortest response time 20 s of yaw rate and fastest response of 22 s of assist current. Vehicle yaw rate is decreased by 1 deg and step response of assist current is decreased to 3 A after adding limitations.

(2) Reliability of the return control strategy is verified by the performance test bed and vehicle test. In this way, return current decreases with an increase of vehicle speed. Return residual angle of the system declines significantly after adding return control. Return response time is shorter and return overshooting decreases, thereby improving the control stability of vehicles.

This study constructs a predictive control model of vehicle EPS and proposes the return control strategy of steering wheel. The proposed model can improve control stability of vehicles. This method can be applied to return simulation and theoretical modeling studies of different vehicles. Given that driving conditions are complicated and changing, future studies can use road excitation as control parameters and formulate control strategies applicable to

different road conditions. This aspect is the key point in future studies.

References

1. Zhao, Q., Zhu, B., Pei, Y. et al., "Integrated control of electric power steering and active suspension systems based on model predictive algorithm." *International Journal of Applied Electromagnetics and Mechanics*, 65(2), 2020, pp. 1-21.
2. Zheng, X., Zhu, L., Luo, J., et al., "Simulation analysis of electric power steering System (EPS) test platform." *Journal of Physics: Conference Series*, 1732(1), 2021, pp. 012193-012199.
3. Lee, J., Chang , H. J., Ahn, H. S., "Explicit MPC for column-type EPS systems." *IET Electric Power Applications*, 14(1), 2020, pp. 91-100.
4. Li, Z., Shi, S., "Stability of EPS system of agricultural vehicles under vibration environment." *INMATEH-AGRICULTURAL ENVIRONMENT*, 1(51), 2017, pp. 101-110.
5. Li, S., Zong, C.,Wu, Z., et al., "Active return-to-center control method for electric power steering." *Journal of Jilin University* (*Engineering and Technology Edition*), 46(2), 2012, pp. 1355-1359.
6. Na, S., Li, Z., Qiu, F. et al., "Torque Control of Electric Power Steering Systems Based on Improved Active Disturbance Rejection Control." *Mathematical Problems in Engineering*, 2020(6), 2020, pp. 1-13.
7. Chen, J., Guo, Y., "Research on Control Strategy of the Electric Power Steering System for All-Terrain Vehicles Based on Model Predictive Current Control." *Mathematical Problems in Engineering*, (3941), 2021, pp. 1-15.
8. Li, Y., Feng, Q., Zhang, Y., "Dual-Motor Full-Weight Electric Power Steering System for Commercial Vehicle." *International Journal of Automotive Technology*, 20(3), 2019, pp. 477-486.
9. Ding, L., Liu, R., YIN, S., "Modeling and optimal design on electric power steering of electric vehicle." *Computer Simulation*, 36(04), 2019, pp. 78-82.
10. Wang, S., Shi, G., Zhang, H., "Active disturbance rejection control of steering wheel torque in integrated electric-hydraulic steering system." *Automobile Engineering*, 43(05), 2021, pp. 770-775+790.
11. Ma, Z., Zhou, H., Li, X., "The research on electric vehicle EPS system reliability based on MDA." Automobile Technology, (12), 2020, pp. 36-42.
12. Shang, X., Lin, M., Tong, L., "Research on control strategy of EPS system based on carsim light truck." *Computer Simulation*, 38(01), 2021, pp. 129-133.
13. Masahiko, Kurishige., Hideyuki, Tanaka., Noriyuki, Inoue., "EPS control strategy to improve steering maneuverability on slippery roads." *In: SAE World Congress & Exhibition, Detroit,* USA: SAE, 2002, pp.1-8.
14. Yoshiyuki, Yasui., Wataru, Tanaka., Yuji Muragishi., "Estimation of lateral grip margin based on self-aligning torque for vehicle dynamics enhancement." *In: SAE World Congress & Exhibition, Detroit,* USA: SAE, 2004, pp. 9-18.
15. Chen, J., Zhao, L., Zu, S., "EPS return control based on fuzzy NLSEF control method." *Journal of Hefei University of Technology (Natural Science)*, 5(40), 2017, pp. 595-600.
16. Wang, Q., Wang, J., Chen, W., "Returnability control strategy for EPS based on vehicle sideslip angle." *Automotive Engineering,* 8(37), 2015, pp. 910-91.
17. Du, P., Su, H., Tang, G., "Active Return-to-Center Control Based on Torque and Angle Sensors for Electric Power Steering Systems." *Sensors*, 18(3), 2018, pp. 855-867.
18. Li, M., "Research on estimation algorithms of tire slip angle and road tire friction coefficient vehicle with steering-by-wire." Master thesis of Jilin University, China, 2011, pp. 8-9.
19. Gong, J. W., Jiang, Y., Xu, W., "Model predictive control of unmanned vehicle." Beijing: Beijing Institute of Technology Press, China, 2014, pp. 49-50.